

Packing structure of a two-dimensional jamming granular system

Xiang Cheng¹

¹*The James Franck Institute and Department of Physics,
The University of Chicago, Chicago, Illinois 60637, USA*

(Dated: January 26, 2023)

We performed a novel experiment on granular packs composed of automatically swelling particles. By analyzing the Voronoi structure of packs going through the jamming transition, we show that the local configuration of a jamming pack are strikingly similar to that of the glass-forming liquids, both in terms of their universal area distribution and the process of defect annealing. Furthermore, we demonstrate that an unambiguous structural signature of the jamming transition can be obtained from the pair correlation functions of a pack. Our study provides insights into the structural properties of general jamming system.

PACS numbers: 81.05.Rm, 61.43.Fs, 83.80.Fg

Nearly 300 years ago, the reverend English scientist Stephen Hales designed a clever experiment to investigate the packing structure of spherical particles [1]. He put spherical peas into a fixed-volume jar filled with water. Absorbing the water slowly, the peas confined in the jar swelled up and deformed under the enormous stress of swelling. From the shape of deformed peas, Hales deduced the structure of the initial pea pack. Though Hales might not realize it, his classic experiment provides an excellent way to probe the jamming transition of a granular pack. In this letter, we report a two dimensional (2D) version of Stephen Hales' experiment. From the position of swelling particles in a cell of fixed area, we investigated the structure of a granular pack evolving continuously through the jamming transition.

Jamming transition and the jamming phase diagram [2, 3], as intriguing concepts for unifying transitions of diverse systems ranging from granular matter to molecular glass, have attracted intensive interests recently [3, 4, 5, 6, 7, 8]. It has been found that an athermal granular system near the jamming point has unique and peculiar behaviors. However, most of these results are only obtained in theories and simulations for ideal systems of frictionless spherical particles. How to extend the theoretical and simulation results to experimental granular system with frictional contact is not straightforward. While Majmudar *et al.* found the increasing of the average coordination number of particles and the pressure of the system agree with the mean-field theory of frictionless particles [9], the results of other experiments contradict the results of simulations [10, 11, 12]. Moreover, very few experiments directly investigated the structural signature of the jamming transition. Corwin *et al.* indirectly deduced the structural signature of the transition from the statistics of the contact forces between particles [13]. Other than granular system, Zhang *et al.* investigated the structural signature of a colloidal system at finite temperature [14].

Here, we experimentally study the structure of a granular pack going through the jamming transition. Instead

of peas, we used tapioca pearls as our granular material. Tapioca pearls are spherical balls made of starch. They can also swell up by absorbing water. The average diameter of dry pearls is $d_0 = 3.3\text{mm}$ with the polydispersity of 8%, which prevents the system from forming large crystalline areas. A fully swelled particle can be as large as 1.7 times of its original size, which leads to almost 3 times increases in packing fraction (ϕ) of a 2D system. More importantly, the swelling of pearls is slow and uniform. Pearls keep spherical shape during swelling. A single layer of pearls are laid down randomly into a squared cell with the side length of 54.6cm. The vertical height of the cell is kept at 5.454mm, which prevents fully swelled pearls from buckling into two layers. The cell can hold over 15,000 particles at the initial packing fraction $\phi_0 \gtrsim 0.63$. A subset of the sample (about 10,000 particles) is studied in the central area of the cell to avoid the possible boundary effect. To allow the pearls to swell, the whole system including the cell and particles is submerged under water. A high resolution camera is used to take an image of the sample every 20s. Due to the slow swelling of pearls, the system is quasi-stationary at this time scale. The acquired images are then analyzed with a particle tracking algorithm [15]. The center of particles can be determined with an error of 0.1mm (about 3% of a particle diameter). A 2D projection of images is used to obtain ϕ of the system. More details of the experiment can be found in [16].

We prepared the sample initially at a dense but un-jammed state. As the size of particles increases, the system goes through the jamming transition and is eventually trapped inside the jammed phase. We constructed a Voronoi tessellation from the centers of particles for each image with increasing ϕ . A Voronoi cell of a particle is defined as the polygon whose interior is closer to the center of the particle than to centers of any other particles, which reveals the local configurations of packing [1].

We first studied the area distribution of the Voronoi cells, $P(s)$, at different ϕ as the system going through the jamming transition. We choose the scaling previ-

ously used to analyze the structure of glass-forming liquids [17]. The area of cell s is shifted by the average area $\langle s \rangle$ and is scaled by its standard deviation σ_s , *i.e.* $\bar{s} = (s - \langle s \rangle) / \sigma_s$. The probability distribution function is then $P(\bar{s}) = \sigma_s \cdot P(s)$ (Fig. 1). The shape of normalized distributions at small ϕ depends on the initial random configuration of particles (Fig. 1a), which varies for each run. However, as ϕ increases toward the jamming point, we found that all $P(\bar{s})$ collapse into a single master curve. To show the detail, we plot the collapsed $P(\bar{s})$ separately in Fig. 1b and also show them in a log-linear plot in the inset of Fig. 1b. It is surprising that all the packs with ϕ ranging continuously from 0.83 up to 0.90 (which is the upper limit of our experiment due to the finite swelling potential of particles under compression) follow the same universal distribution. From the structural signature of the jamming transition which we shall show later, we know that the system jams at $\phi \simeq 0.84$. Hence, the universal distribution emerges only close to and after the jamming transition. It should be emphasized that the universal distribution for this large range of ϕ is non-trivial: the jammed phase of a pack is far from stationary. Though particles is confined by their neighbors, the shape of Voronoi cells is highly mobile as illustrated below. Some localized collective particle rearrangement also exists in the jammed phase [16].

Quantitatively, we fitted the universal distribution with a shifted gamma distribution (Fig. 1b),

$$P(\bar{s}) = (\bar{s} - \bar{s}_0)^{k-1} \frac{\exp(-(\bar{s} - \bar{s}_0)/\theta)}{\Gamma(k)\theta^k}, \quad (1)$$

where θ and k are standard parameters of gamma distribution and \bar{s}_0 is a fitting parameter since the shift in s axis. The same distribution has been suggested previously in [18, 19]. We also compare the gamma distribution with a Gaussian distribution (Fig. 1b). Due to the asymmetric shape of the distribution, the gamma distribution gives a better description of our data.

Disorder and geometric constraint are two salient features of the jamming transition and the basic organizing themes underlying the jamming phase diagram. Both of them are essential in determining the shape of the universal distribution, which can be seen as following. First, it is evident that for an order structure the area distribution of Voronoi cells should be a delta function (or delta functions). Second, we compare the distribution of our jamming system with that of totally random points without any geometric constraint of particle size (Fig. 1b). For random points, the peak of the distribution shifts to the left and the distribution are biased toward right.

It has already been found that the Voronoi structure of glass-forming liquids also follows a universal distribution at different temperatures (T) ranging from liquid states to supercooled states [17]. Even more striking, the universal distribution of the Voronoi structure of

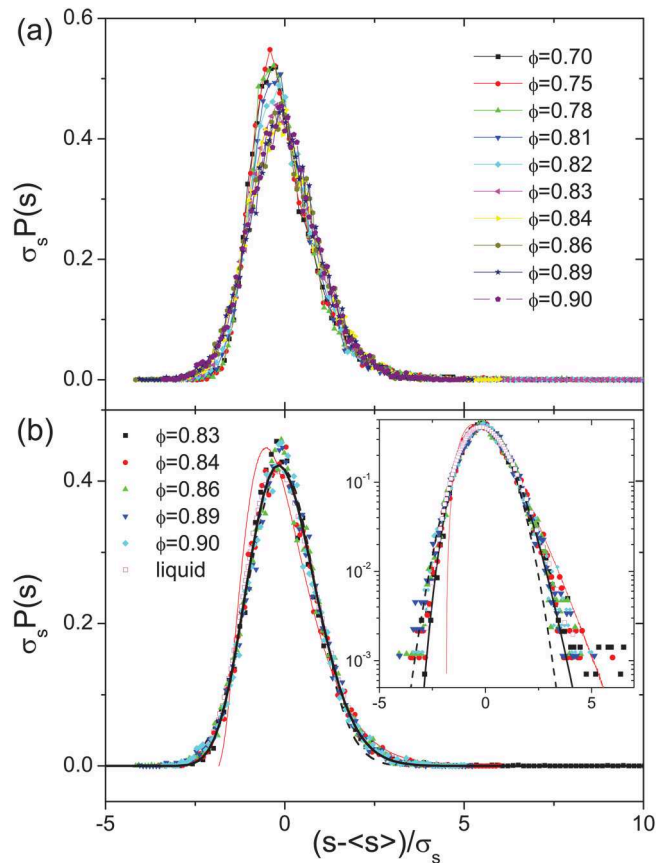


FIG. 1: (color online). Distribution of Voronoi cell areas, shifted by the average area and scaled by its standard deviation. (a) Distribution for a pack with ϕ increasing from 0.70 to 0.90. (b) The collapse of the distributions near and after the jamming transition. The universal distribution of Voronoi structure of the glass-forming liquids (empty magenta squares) is taken from [17]. The thick black line is the gamma distribution with $k = 30$, $\theta = 0.175$ and $\bar{s}_0 = -5.3$. The black dashed line is a Gaussian fit. The thin red line is the distribution of Voronoi structure of random points. The inset is the log-linear plot of the same data.

glass-forming liquids is *quantitatively* similar to the universal distribution of our 2D jamming granular system (Fig. 1b). It is likely that near the glass transition the interaction between molecules of a supercooled liquid is dominant by its strong repulsive potential, therefore like the athermal granular system the geometric constraint of the molecules determines the local configurations and its distribution. In addition, it is noted that deep inside the jammed phase the area distribution is invariant, which is consistent with previous study of the Voronoi structure of static granular packs at several discrete ϕ [18]. Here, we show the invariant distribution with ϕ varying continuously and uniformly in a larger range. The universal distributions of Voronoi structure in glass-forming liquids at different T and in a granular system going through the jamming transition at different ϕ corroborate the con-

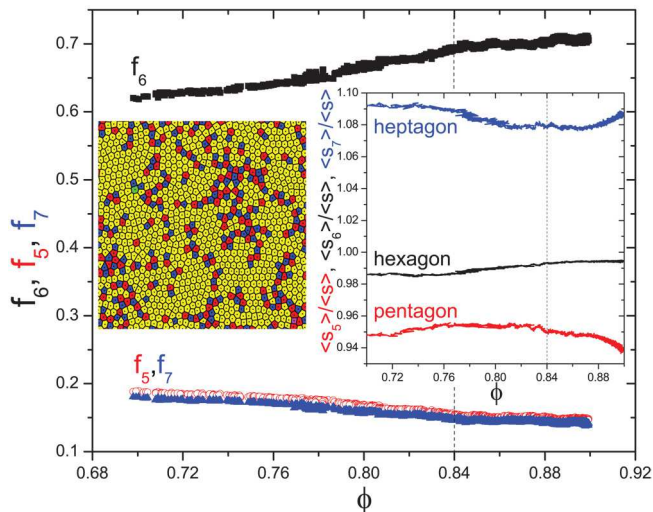


FIG. 2: (color online). Main plot: Number fraction of different type of cells with increasing ϕ . Black squares for hexagons (f_6), red circles for pentagons (f_5) and blue triangles for heptagons (f_7). Left inset: Shape of cells in Voronoi tessellation of a pack at $\phi = 0.86$. Yellow cells are hexagons; blue cells are pentagons and red cells are heptagons. There is also one octagon (green) and one square (magenta). Note that most of pentagons and heptagons join into neighboring pairs and can anneal to hexagons later. Right inset: the average area of hexagons, pentagons and heptagons over the total average area of cells. The vertical dashed lines in both plots indicate the jamming point obtained from the structural signature of the jamming transition explained in the text.

cept of the jamming phase diagram [2]. In respect to the Voronoi structure, T -axis and $1/\phi$ -axis of the phase diagram are equivalent. We conjecture that all the jamming systems near the jamming point show a qualitatively similar universal distribution of local configurations.

We also investigate the shape of Voronoi cells. In 2D, the geometric Euler constraint implies that average number of edges of a cell should be 6 [1, 20]. Cells with the number of edges other than 6 are usually referred to as “defects” [20, 21, 22]. We count the fractions of pentagons, hexagons and heptagons in the system (f_5, f_6 and f_7), as it goes through the jamming transition. As shown in Fig. 2, f_6 increases while f_5 and f_7 decrease: with increasing ϕ , a pair of pentagon and heptagon can anneal to two hexagons. It is interesting that the annealing process continues even at ϕ clearly above the jamming point: the shape of the Voronoi cells is highly mobile with only tiny deformation of particles inside the jammed phase. Nevertheless, the annealing slows down deep inside the jammed phase and stops eventually. Due to the disordered nature of the jammed phase, a finite amount of the pentagon/heptagon pairs persists [20].

It has been proposed that the glass transition of binary-mixture molecular liquids can be characterized by the disappearance of certain kinds of “liquid-like” defects

(heptagons enclosed small molecules and pentagons enclosed large molecules) in Voronoi tessellation [21, 22]. It is possible that in our granular system the “liquid-like” defects diminish during annealing and the remaining defects inside jammed phase are associated with “glass-like” defects. Due to the continuous distribution of the size of our particles and the difficulty to measure the accurate size of particles under water, we cannot directly verify the above scenario. However, a consistent check can be made by analyzing the average area of different types of cells. If heptagons enclosed small molecules, which should have smaller Voronoi cells in a condensed phase on average, diminish, then the average area of heptagons normalized by the total average area, should increase. Similarly, if pentagons enclosed large molecules disappear, the average area of pentagons over the total average area should decrease. Here, we measured the average area of pentagons, hexagons and heptagons normalized by the total average area of all cells, $\langle s_{5,6,7} \rangle / \langle s \rangle$, as a function of ϕ (Fig. 2 right inset). First, we can see pentagons have smaller area on average ($\langle s_5 \rangle / \langle s \rangle < 1$) and heptagons have larger area on average ($\langle s_7 \rangle / \langle s \rangle > 1$). The trends of $\langle s_{5,6,7} \rangle / \langle s \rangle$ are more interesting. Before jamming the trends depend on the initial packing configuration of individual experiment, similar to the behavior of $P(\bar{s})$ before jamming. However, close to and after the jamming transition the features of $\langle s_{5,6,7} \rangle / \langle s \rangle$ are robust for all experiments: $\langle s_6 \rangle / \langle s \rangle$ plateaus, but $\langle s_5 \rangle / \langle s \rangle$ clearly decreases and $\langle s_7 \rangle / \langle s \rangle$ increases. This is exactly what we expected from the behavior of glass-forming liquids [21, 22].

Before we can explore the relation between the glass transition and the jamming transition further, we need to ask a simple but important question: where does an athermal system jam? Though the jamming point of a pack can be identified by its mechanical properties [3], experimentally it is usually hard to acquire further information of a pack except the position of all its particles. Can we detect the jamming transition from just the structure of a pack? Despite the interesting features shown above, the Voronoi tessellation does not provide a unambiguous standard of the jamming transition. Both the area distribution and the annealing of defects show only quantitative change before and after transition. We shall show next that the pair correlation of a pack provides a structural signature of the jamming transition.

We plot the pair correlation functions, $g(r)$, of a pack at different ϕ through the jamming transition (Fig. 3). At each ϕ , $g(r)$ has an oscillating shape, typical for amorphous packs of spherical particles. Peaks in $g(r)$ indicate the layering structure of the pack, the positions of which shift to larger r as ϕ increases since the enlargement of particles. A structural signature of the jamming transition can be obtained by measuring g_1 , the height of the first peak of $g(r)$. $g_1(\phi)$ shows a non-monotonic behavior with a peak at $\phi^* = 0.84 \pm 0.02$ (Fig. 3 inset). We also measured the force applied by the pack on the boundary

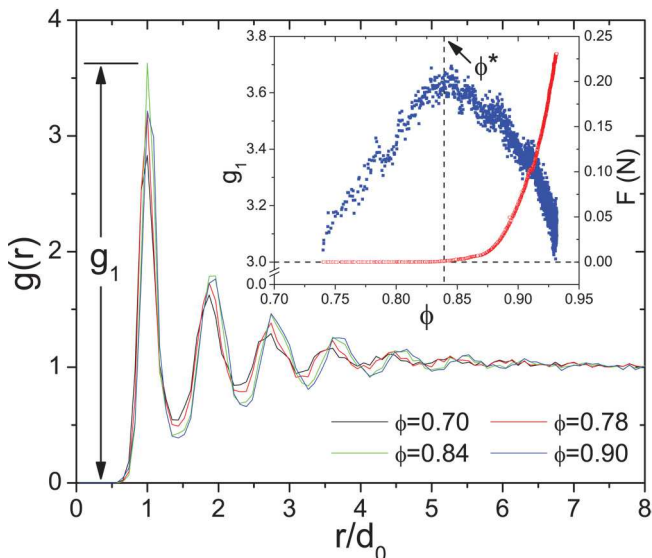


FIG. 3: (color online). Pair correlations of a pack at different ϕ . r is normalized by the original size of pearls d_0 . The height of the first peak, g_1 , is indicated. Inset: The height of the first peak $g_1(\phi)$ (blue squares) and the force measured at the boundary of the cell $F(\phi)$ (red circles). The vertical dashed line indicates the peak of $g_1(\phi)$, ϕ^* . The horizontal dashed line indicates the zero force.

of the cell (Fig. 3 inset). The jamming point of the system is marked by the emergence of a non-zero force on the boundary, which is coincident with the peak of $g_1(\phi)$. Hence, $g_1(\phi)$ provides a clear structural signature of the jamming transition and ϕ^* is the jamming point.

The non-monotonic behavior of $g_1(\phi)$ can be seen as the vestige of the structural singularity uncovered in the jamming transition of ideal monodisperse frictionless particles [4]. As a system evolves from unjammed state toward ϕ^* , particles are pushed closer to each other. The distribution of the distance between neighboring particles becomes narrower and g_1 therefore increases. For monodisperse frictionless particles, due to the finite range repulsive interaction, at ϕ^* the distances between contact particles are all exactly one particle diameter. Hence, g_1 , representing the probability to find a neighboring particle at a fixed distance, diverges. Above ϕ^* , due to the disordered nature of the pack, particles will experience different compression and deform differently depending on their local environment. The distances between contact particles spread out again. Quantitatively, $g_1 \cdot w = z$ above jamming, where w is the width of the left hand side of the first peak of $g(r)$ and z is the average coordination number of particles [4]. Since z increases slowly, it can be treated approximately as a constant near ϕ^* . Hence, as w increases from zero above ϕ^* , g_1 decreases. The polydispersity of our particles depresses the divergence in g_1 . Even at ϕ^* , the distribution of the distances between contact particles still has a finite width. Nevertheless, a

maximum of $g_1(\phi)$ is preserved as a vestige of the singularity. Frictional contacts may complicate the situation further [16]. A similar thermal vestige of the structural singularity has also been observed in a colloidal system of finite T [14], where the structural singularity is depressed by the thermal motion instead.

By analyzing the Voronoi tessellation and the pair correlation functions of a granular pack with increasing ϕ , we investigated the structures of the jamming transition. We showed that the local configurations of a jamming granular pack is similar to that of glass-forming liquids, and therefore demonstrated the relation between jamming transition and glass transition in the spirit of the jamming phase diagram. Further study of the local structure of other jamming system, such as the glassy colloidal suspensions or jammed foams, may shed more light on the universal properties of the jamming structure illustrated here. Moreover, we showed that a structural signature of the jamming transition can be obtained from the first peak of pair correlation functions. Our study shows that, though the presence of the realistic conditions such as frictional contacts and non-perfect spherical shape of particles, the structural signature of the ideal jamming system persists in the real experiment.

I thank S. Nagel and H. Jaeger for their support and guidance. I am also grateful to E. Brown, N. Keim, J. Royer, N. Xu and L.-N. Zou. This work was supported by the NSF MRSEC, the Keck foundation and DOE.

-
- [1] T. Aste and D. Weaire, *The Pursuit of Perfect Packing* (Taylor and Francis, New York, ed. 2, 2008).
 - [2] A. J. Liu and S. R. Nagel, *Nature* **396**, 21 (1998).
 - [3] C. S. O'Hern *et al.*, *Phys. Rev. E* **68**, 011306 (2003).
 - [4] L. E. Silbert *et al.*, *Phys. Rev. E* **73**, 041304 (2006).
 - [5] W. G. Ellenbroek *et al.*, *Phys. Rev. Lett.* **97**, 258001 (2006).
 - [6] P. Olsson and S. Teitel, *Phys. Rev. Lett.* **99**, 178001 (2007).
 - [7] S. Henkes and B. Chakraborty, *Phys. Rev. Lett.* **95**, 198002 (2005).
 - [8] M. Wyart *et al.*, *Phys. Rev. E* **72**, 051306 (2005).
 - [9] T. S. Majmudar *et al.*, *Phys. Rev. Lett.* **98**, 058001 (2007).
 - [10] X. Jacob *et al.*, *Phys. Rev. Lett.* **100**, 158003 (2008).
 - [11] L. Bonneau *et al.*, *Phys. Rev. Lett.* **101**, 118001 (2008).
 - [12] M. M. Bandi *et al.*, arXiv:0910.3008 (2009).
 - [13] E. I. Corwin *et al.*, *Nature* **435**, 1075 (2005).
 - [14] Z. Zhang *et al.*, *Nature* **459**, 230 (2009).
 - [15] J. C. Crocker and D. G. Grier, *J. Colloid Interface Sci.* **179**, 298 (1996).
 - [16] X. Cheng, arXiv:0905.2788 (2009).
 - [17] F. W. Starr *et al.*, *Phys. Rev. Lett.* **89**, 125501 (2002).
 - [18] T. Aste *et al.*, *Europhys. Lett.* **79**, 24003 (2007).
 - [19] V. S. Kumar and V. Kumaran, *J. Chem. Phys.* **123**, 114501 (2005).
 - [20] D. N. Perera and P. Harrowell, *Phys. Rev. E* **59**, 5721

- (1999).
- [21] E. Aharonov *et al.*, Europhys. Lett. **77**, 56002 (2007).
- [22] H. G. E. Hentschel *et al.*, Phys. Rev. E **75**, 050404 (2007).